Journal of Materials and Environmental Science
ISSN : 2028-2508
e-ISSN : 2737-890X
CODEN : JMESCN

J. Mater. Environ. Sci., 2024, Volume 15, Issue 12, Page 1776-1795

http://www.jmaterenvironsci.com

Bark Extract of *Urena lobata* as Green Corrosion Inhibitor for Mild Steel in Sulphuric Acid Environment

Enyinnaya N. P.[1]*, James A. O. [1], Obi C.[1]

[1]*Department of Pure and Industrial Chemistry, Faculty of Science, University of Port Harcourt, Port Harcourt, Nigeria.*

**Corresponding author, Email address: nwojo.enyinnaya2@gmail.com*

Received *25 Nov 2024,*
Revised *15 Dec 2024,*
Accepted *17 Dec 2024*

Keywords:
✓ Urena lobata*;*
✓ corrosion inhibition*;*
✓ adsorption mechanism*;*
✓ phytochemical*;*
✓ surface morphology.

Citation: *Enyinnaya, N. P., James, A. O., Obi C. (2024) Bark Extract of Urena lobata as Green Corrosion Inhibitor for Mild Steel in Sulphuric Acid Environment, J. Mater. Environ. Sci., 15(12), 1776-1795*

Abstract: *Urena lobata* bark extract (ULBE) was investigated as corrosion inhibitor for mild steel in 0.5 M H_2SO_4 by phytochemical method, gravimetric and surface morphological studies. Phytochemical screening revealed the presence of alkaloids, flavonoids, saponins and other phytochemicals that inhibit corrosion. The result showed that inhibition efficiency increases with concentration of the inhibitor (from 0.2 g-1.0 g) reaching maximum of 96.82 % at 303 K and 24 hr immersion time. It also decreases with temperature rise from 303 K to 333 K. The thermodynamic parameters obtained support a physical adsorption mechanism and best fitted to the Langmuir adsorption isotherm. The values of activation energies obtained in the presence of the inhibitor was all higher than that of the blank solution indicating that ULBE inhibitor effectively inhibits mild steel corrosion. The inhibition process followed first order kinetics. Surface morphological studies revealed that the inhibited mild steel coupons have smooth surfaces whereas mild steel immersed in blank solution showed rough and irregular surfaces, hence confirming the inhibition ability of the inhibitor.

1. Introduction

Corrosion is an extremely demanding challenge in industrial chemical processes and is a factor in installation components and material failure due to a chemical or electrochemical attack from the environment (Popov (2015); Revie & Unlig, (2018)). Mild steel is used in general engineering constructions and in the oil and gas industries due to its reasonable price and mechanical strength advantage. Sulphuric acid is often used in performing acid descaling, acidizing and acid pickling in oil wells to enhance oil recovery (Guo *et al*. 2017; Bouklah *et al*. 2006a). However, this acid may corrode the surface of the mild steel resulting in significant costs for renovation and system maintenance, as well as physical and environmental losses (Hannon *et al*. 2021). Researchers have established the use of corrosion inhibitors in retarding corrosion of metals (Ma *et. al*. (2021); Umoren *et al*. (2022); Akpan *et al*. (2024)). An inhibitor is a substance (or a combination of substances) added in a very low concentration to treat the surface of a metal that is exposed to a corrosive environment in order to terminate or diminish the corrosion of a metal (Chetouani *et al*. (2004); Ghazi *et al*. (2014); Ngobiri & Obi, (2020)). The inhibitors like plant extracts presumably possess biocompatibility due to their biological origin. Many researchers have studied the inhibitive performance of various root extracts of

plants. Researchers like (Awe *et al*. (2015); Haldhar *et al*. (2018); Feng *et al*. (2021)) successful investigated the use of root extracts of bitter leaf, beet, *Valeriana willichi* and vetratum as corrosion inhibitors of metals in harsh environment. There is still growing need to exhaustively utilized biodegradable plant parts extracts in the protection of metal surfaces in the presence of toxic environments. In this study, the effects *Urena lobata* bark extract on the corrosion inhibition of mild steel in 0.5 M H_2SO_4 was investigated using gravimetric method and surface analysis techniques.

2.0 Methodology

2.1 Sourcing and preparation of the plant sample

Fresh samples of *Urena lobata* barks were collected from a farm in Mbodo Aluu (Lat. 4.9339°N, Long. 6.9437°E) in Ikwerre L.G.A. of Rivers State, South-South, Nigeria. The plant was taxonomically identified in Herbarium of Plant Science and Biotechnology Department, University of Port Harcourt, Nigeria where a voucher specimen was also deposited. The plant parts were washed with tap water, rinsed twice with distilled water, and air-dried to constant weight under shade at room temperature for a week. The dried samples were ground to powder using electric grinding machine. A 100 g of dry sample was extracted by maceration for 3 days in 1000 cm^3 beaker containing 500 cm^3 of methanol. The mixtures were filtered using and the solvent evaporated using rotary evaporator at 70°C to concentrate the extracts. The stock solution of the extracts obtained was used in preparing different concentrations of the *Urena lobata* bark extract (ULBE). Inhibitor solutions were prepared by weighing the correct mass of the inhibitors (0.2 g, 0.4 g, 0.6 g, 0.8 g, and 1.0 g) and then dissolved in 0.5 M H_2SO_4 solution and made up to 1000 cm^3 to obtain 0.2 g/L, 0.4 g/L, 0.6 g/L, 0.8 g/L and 1.0 g/L inhibitors solution. The blank solution used was 0.5 M H_2SO_4 corrodent solution without the inhibitors added. Mild Steel (MS) sheet was obtained from Metal section of Mile 3 Market Port Harcourt, Rivers State, Nigeria. The Metal Sheet was press-cut into coupons of dimension 2 cm x 3 cm x 1.5 mm for mild steel in Science and Engineering Workshop (SEW), Choba Campus, University of Port Harcourt. The coupons were polished mechanically using emery paper, washed with distilled water, degreased with ethanol and acetone, dried at room temperature, and stored in a moisture-free desiccator prior to use. The elemental composition of the mild steel coupons used for this study as analyzed using optical electronic spectroscopy (OES) is as follows: C (0.2300%), Mn (0.2654%), Cr (0.0528%), Co (0.0313%), Ni (0.2205%), Cu (0.2120%), Mo (0.0330%), Si (0.0547%) and the rest Fe.

2.2 Weight Loss Experiment

Weight loss experiments were conducted under total immersion conditions in 250 ml of test solution, maintained at 303 K, 313 K, 323 K and 333 K for 24-168 hr. The test coupons which were weighed before immersion and were retrieved at the end of the specified time, scrubbed with bristle brush under tap water until clean. The clean test coupons were rinsed in ethanol, dried in acetone, and reweighed. All tests were run in triplicate, and average values were obtained and used in subsequent calculations. The weight loss was taken as the difference between the weight of coupon before and after immersion (Enyinnaya *et al*. (2021)). From the weight loss data, corrosion rate was calculated using equation 1:

$$\mathbf{C_R = \frac{534\Delta w}{DAt}} \qquad 1$$

Where C_R is the corrosion rate in Mills per year penetration (MPY), D, density of sample/coupon in g/cm^3, A, is the surface area of the coupon in cm^3, t, is exposure time in hours and ΔW represents

weight loss in mg. The inhibition efficiency (IE%) and the degree of surface coverage (θ) of the extract were calculated by comparing the weight loss in the absence and presence of each inhibitor in the test solutions studied using the relationship in equations 2 and 3 as reported by (Saeed *et al*. (2019)).

$$IE\ \% = \left(1 - \frac{C_{R(in)}}{C_{R(bl)}}\right) x\ 100 \quad (2)$$

$$\theta = \left(1 - \frac{C_{R(in)}}{C_{R(bl)}}\right) \quad (3)$$

Where $C_{R(in)}$ and $C_{R(bl)}$ are the weight loss for the inhibited solution and blank solution respectively.

2.3 Product characterisation

2.3.1 Phytochemical Studies

Phytochemical analysis of methanolic *Urena lobata* bark extract was carried out using standard procedures according to the method reported by (Banu & Cathrine, 2015).

2.3.2 Scanning Electron Microscopy (SEM)

Surface morphology and texture of the coupons were analyzed using Scanning Electron Microscopy (SEM) (Model-PHENOM ProX). Surface analysis of mild steel was analyzed using SEM before and after immersion in inhibited and blank solutions at 303 K after 168 hr.

2.3.3 Fourier Transformation Infra-red (FTIR) Spectroscopy

The Fourier transform Infra-red (FTIR) analysis of inhibitors and the corrosion products were carried out by a FTIR equipment trademarked SHIMADZU FTIR-8400S incorporated with software (Perkin Elmer Instruments version 3.02.1) for the examination of the spectra. The coupons were exposed in 100 ml 0.5 M H_2SO_4 for inhibited and uninhibited solutions for 24 hr at 303 K washed with distilled water. After washing, the coupons were dried and examined using FTIR for the functional groups adsorbed. The spectra were recorded in the frequency range of 4000 and 400 cm^{-1}.

3.0 Results and Discussion

3.1 Phytochemical Evaluations of Bark Extract of *Urena lobata*

Phytochemical analysis of the extract inhibitor presented in Table 1 revealed the presence of some phytochemicals such as tannins, phenolic compounds, steroids, and alkaloids responsible for the inhibition of corrosion.

3.2 Weight Loss Evaluation

The weight loss of Mild steel coupons in 0.5 M H_2SO_4 in the presence and absence of different concentrations of the inhibitor for a total immersion time of 24 -168 hr were determined at 303 K – 333 K. The weight loss-time plots for mild steel coupons in the extracts from 303 K to 333 K in Figures 1-4 showed that the weight loss of mild steel in the presence of the inhibitor increased with temperature rise leading to decrease in inhibition efficiency. Decreased efficiency of inhibition with temperature rise was due to desorption effect of inhibitor molecule as a result of increase in the solubility of the protective films and reaction products precipitated on mild steel surface that otherwise inhibit corrosion process (Bentiss *et al*. (2009); Santhini *et al*. (2012); Chaubey *et al*. (2012); Diki *et al*. (2018)). This indicates that the adsorption mechanism of *Urena lobata* bark extract on mild steel surface favored the charge transfer from charge inhibitors to charged metal surfaces which supports physical adsorption

(Abakedi *et al*. (2018)). The variations of inhibition efficiency with inhibitor's concentration for mild steel corrosion at varying temperatures from 303 K to 333 K as presented in Figure 6 revealed that the inhibition efficiencies of the inhibitor increased with inhibitor's concentrations but decreased with temperature rise.

Table 1: Phytochemical composition of the *Urena lobata* bark extract (ULBE)

Phytochemical	ULBE inhibitor
Saponins	+
Tannins	+
Flavonoids	+
Alkaloids	+
Phenolic compounds	+
Steroids	+
Reducing sugar	+

+ Presence of phytochemical, - absence of phytochemicals

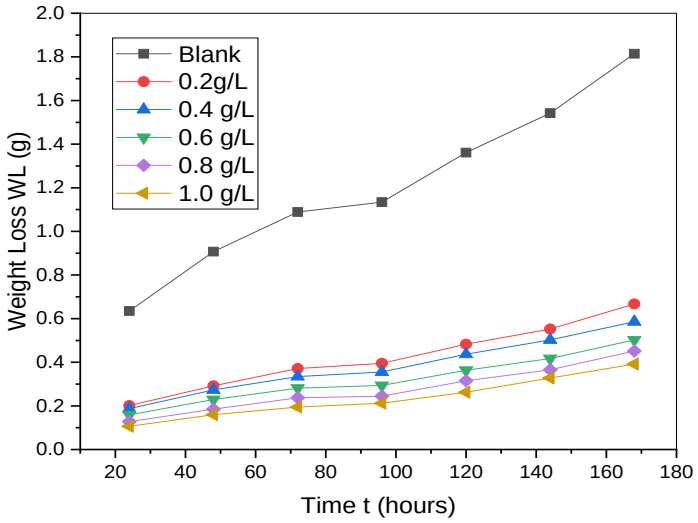

Figure1: Variation of weight loss with time of MS in 0.5 M H_2SO_4 at 303 K in the presence of different concentrations of ULBE

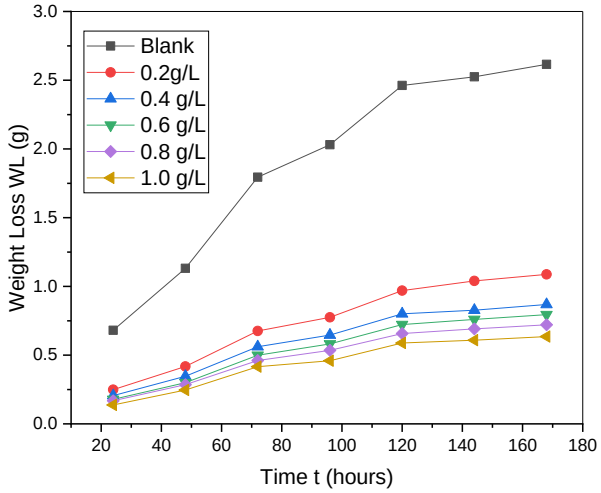

Figure 2: Variation of weight loss with time of MS in 0.5 M H_2SO_4 at 313 K in the presence of different concentrations of ULBE

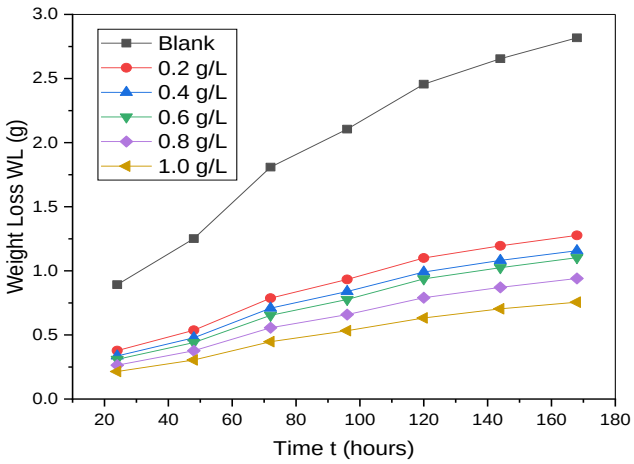

Figure 3: Variation of weight loss with time of MS in 0.5 M H_2SO_4 at 323 K in the presence of different concentrations of ULBE

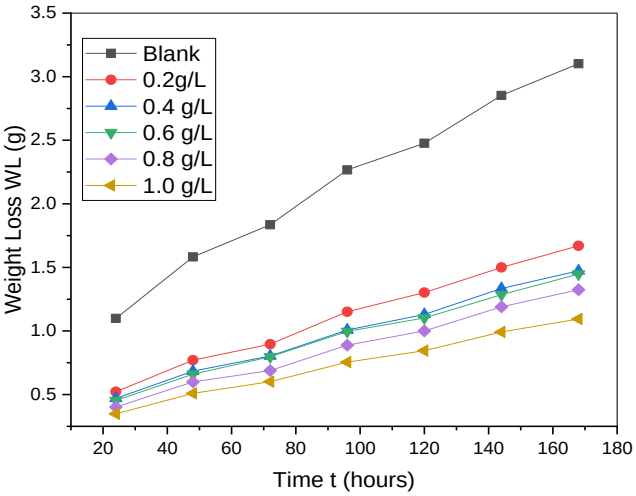

Figure 4: Variation of weight loss with time of MS in 0.5 M H_2SO_4 at 333 K in the presence of different concentrations of ULBE

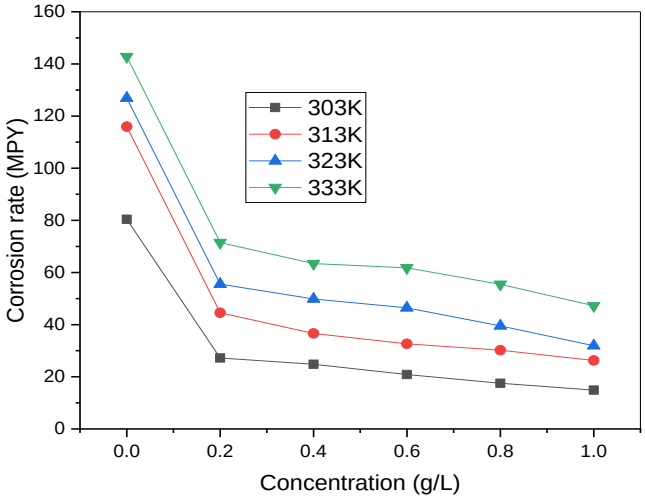

Figure 5: Corrosion rate of MS in various ULBE inhibitor concentrations at different temperatures

The variations of corrosion rate of mild steel with concentrations of the inhibitors as shown in Figure 5 revealed that the corrosion rates of mild steel decreased with increase in inhibitor's concentration. This was due to formation of protective corrosion product films on the surface of the mild steel which inhibit corrosion (Enyinnaya *et al*. (2022); Dhakal *et al*. (2022)).

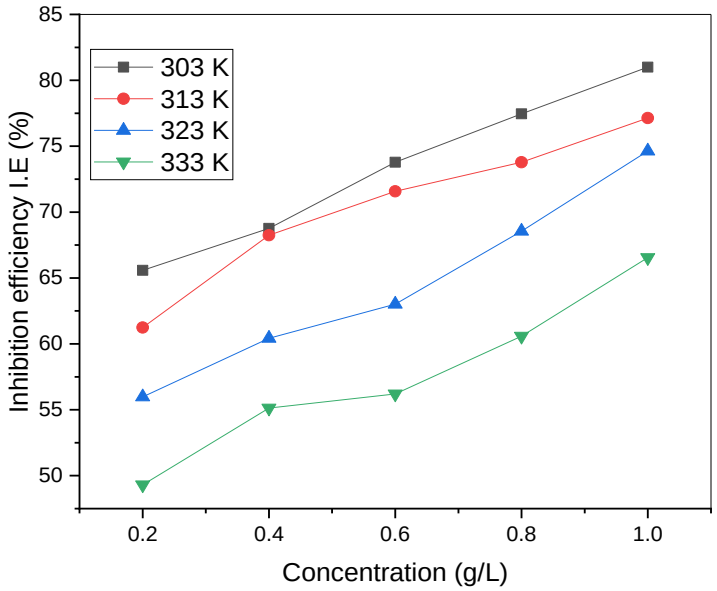

Figure 6: Variation of inhibition efficiency with concentration of ULBE inhibitor for MS corrosion in 0.5 M at H_2SO_4 different temperatures

This result suggests that the increase in efficiencies with increase in inhibitor's concentration was due to increase of the number of molecules adsorbed onto mild steel surface which reduces the surface area that was available for the direct acid attack on the metal surface leading to corrosion (Kazaure *et al*. (2015); Enyinnaya *et al*. (2021)). The obvious decrease in inhibition efficiency with temperature rise could be due to desorption of already adsorbed inhibitor at high temperature (Bentiss *et al*. (2009)).

3.3 Thermochemical Evaluation

The apparent activation energy of the corrosion process in the absence and presence of ULBE inhibitor was obtained using the Arrhenius equation; equation 4.

$$\boldsymbol{log\, C_R = log\, A - \frac{E_A}{2.303RT}} \qquad 4$$

Where E_A the activation energy of the process. A plot of log C_R against $\frac{1}{T}$ gave straight line with coefficient of regression R^2 close to unity as shown in Figure 7. The slope of the graph was given by $-\frac{E_A}{2.303R}$ from which apparent activation energy E_A was obtained while the intercept was given by log A. The apparent enthalpy of activation (ΔH^*) and apparent entropy of activation (ΔS^*) for the activation complex formation in transition state was determined using transition state equation (equation 5) as applied by (Abdallah *et al*. (2019)):

$$\mathbf{C_R = \frac{RT}{Nh} exp\left(\frac{\Delta S*}{R}\right) exp\left(-\frac{\Delta H*}{RT}\right)} \qquad 5$$

Where N is the Avogadro's number, h is the Planck's constant, ΔH^* is the apparent activation enthalpy and ΔS^* is the apparent entropy of activation. A plot of $\log -\frac{C_R}{T}$ against $\frac{1}{T}$ as presented in Figure 8 showed a straight-line plot and the values ΔS^* and ΔH^* obtained from the intercept and slope presented in Table 2. The plots in Figures 7 and 8 showed Arrhenius and Eyring Transition state mechanism in the presence and absence of different inhibitor's concentrations on mild steel inhibition respectively. The activation energies $\mathbf{E_A}$ for inhibited solutions were more than that of uninhibited (blank) solution which gave 15.40 kJ/mol as shown in Table 2. The values of $\mathbf{E_A}$ for ULBE range from 26.33-31.44 kJ/mol. Because $\mathbf{E_A}$ values in the presence of inhibitors were greater than its absence, it shows that mild steel was effectively inhibited by ULBE. However, higher values of $\mathbf{E_A}$ in the presence of inhibitors signify physical adsorption mechanism (Fouda *et al*. (2019)).

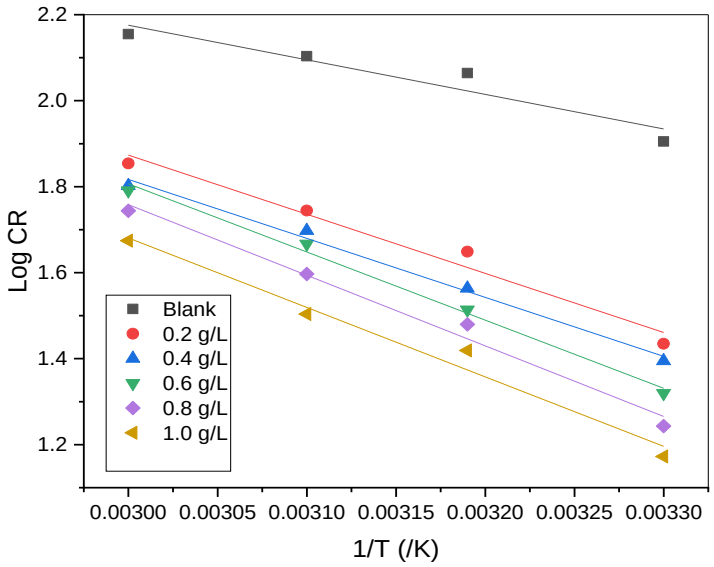

Figure 7: Arrhenius plots in the presence and absence of different concentrations of ULBE on MS inhibition

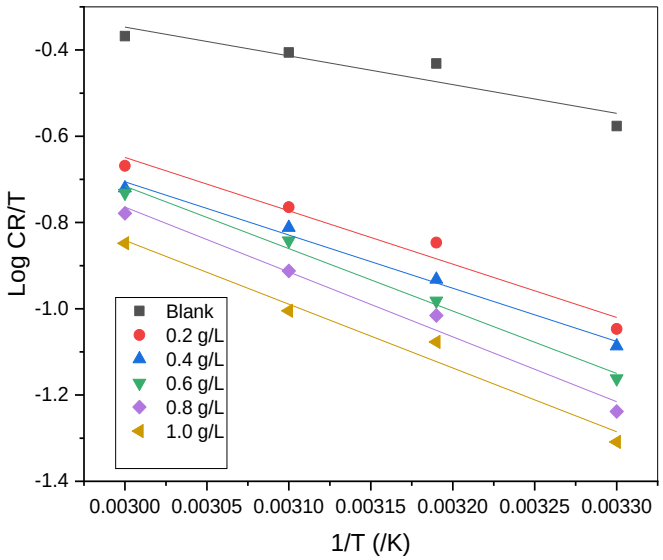

Figure 8: Transition state plots in the presence and absence of different concentrations of ULBE on MS inhibition

Table 2: Corrosion activation parameters for MS in 0.5 M H_2SO_4 in the absence and presence of different concentrations of ULBE inhibitor

Concentration (g/L)	**E_a (kJ/mol)**	**ΔH* (kJ/mol)**	**ΔS* (J/mol/K)**	**ΔG* (kJ/mol)**			
				303 K	313 K	323 K	333 K
Blank	15.40	12.76	-165.93	63.04	64.70	66.36	68.01
0.2	26.33	23.68	-138.96	65.78	67.17	68.56	69.95
0.4	26.26	23.62	-140.24	66.11	67.52	68.92	70.32
0.6	30.35	27.71	-128.17	66.55	67.83	69.11	70.39
0.8	30.93	28.79	-125.83	66.92	68.17	69.43	70.69
1.0	31.44	28.31	-128.75	67.32	68.61	69.90	71.18

The enthalpies of activation (ΔH^*) in the absence and presence of inhibitors was positive indicating the endothermic nature of mild steel dissolution process, meaning that the dissolution was difficult (Ebenso & Obot, (2010)). The activated enthalpy (ΔH^*) values for inhibited solutions in Table 2 were higher than those of uninhibited solution (12.76 kJ/mol) indicating higher protection. This could be due to increase in energy barrier for the reaction due to increase activation enthalpy of corrosion. Apparent activation entropy, ΔS^*, increased in the presence of inhibitors for mild steel corrosion compared to free acid solution. This could be because of the transition state of the rate determining step showing a more orderly arrangement relative to the initial state. For inhibited solutions, the rate determining step was the discharge of H^+ ions to form adsorbed hydrogen atom. Since the metal surface was covered with the inhibitor solution, the discharge of H^+ ion was retarded resulting in a random arrangement hence, increasing the ΔS^*. The negative values of ΔS^* means that the activated complex in the rate determining step represents an association rather than dissolution step. This means that an increase in orderliness took place on going from reactants to the activated complex (Fouda *et al*. (2006); Hammouti *et al*. (2013); Zarrok *et al*. (2013); Fouda *et al*. (2019)).

3.4 Kinetics Evaluation

The plots of variation - log (weight loss) with time for corrosion of mild steel in 0.5 M H_2SO_4 containing various concentrations of the ULBE inhibitor at temperatures 303 K-333 K as presented in Figures 9-12 revealed that the R^2 obtained were close to unity indicating the fitness of these data to pseudo-first order kinetics.

The values of $\boldsymbol{k_1}$, $\boldsymbol{t_{1/2}}$ and R^2 of the inhibitor for mild steel corrosion were recorded in Table 3 and it was evidenced that the rate constant $\boldsymbol{k_1}$, increased while the half-life $\boldsymbol{t_{1/2}}$ decreased with temperature rise for mild steel-inhibitor system. This confirms that the interaction between mild steel and ULBE inhibitor followed physical adsorption mechanism (Bouklah *et al*. (2006b), Ijuo *et al*. (2018); (Kikanme et al. (2020); Enyinnaya et al. (2022)).

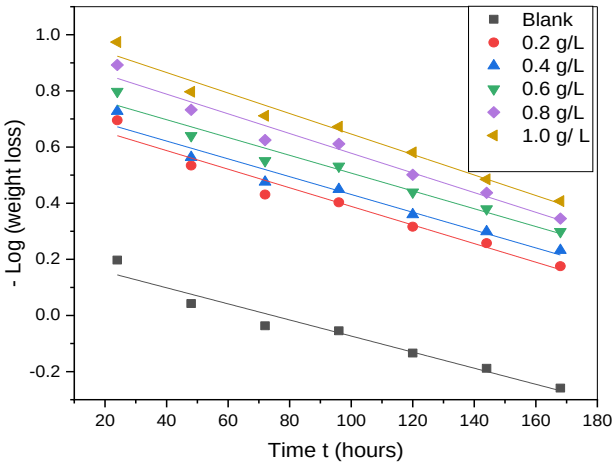

Figure 9: Variation of - log (Weight Loss) with time for corrosion of MS in 0.5 M H_2SO_4 containing various concentrations of ULBE of at 303K

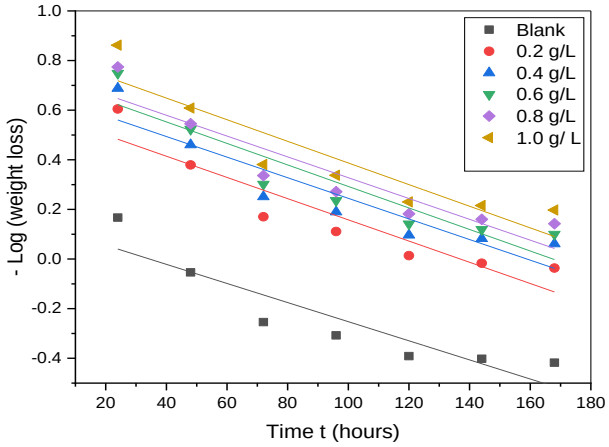

Figure 10: Variation of - log (Weight Loss) with time for corrosion of MS in 0.5 M H_2SO_4 containing various concentrations of ULBE of at 313 K

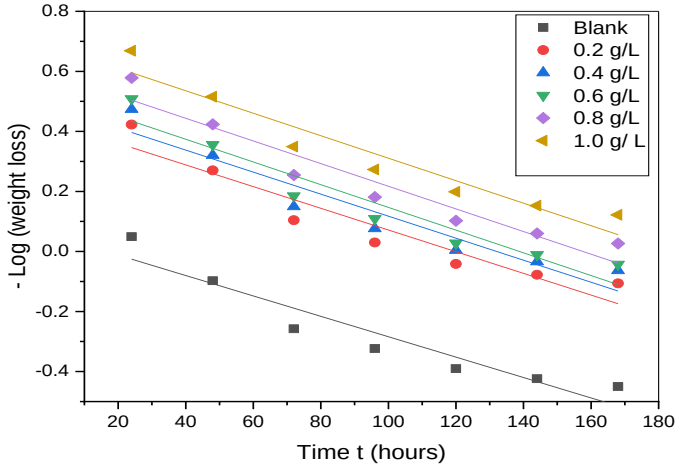

Figure 11: Variation of - log (Weight Loss) with time for corrosion of MS in 0.5 M H_2SO_4 containing various concentrations of ULBE of at 323 K

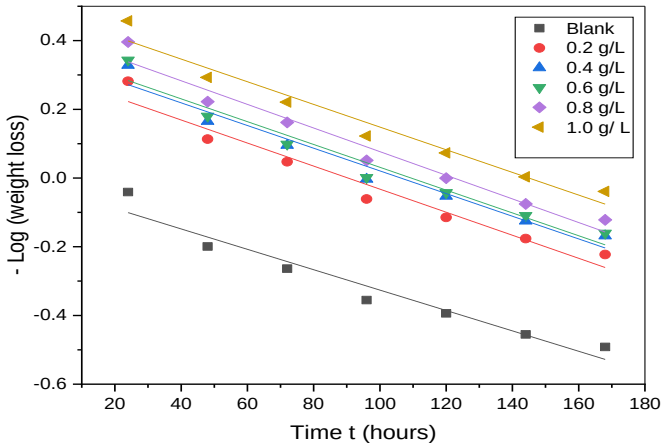

Figure 12: Variation of - log (Weight Loss) with time for corrosion of MS in 0.5 M H_2SO_4 containing various concentrations of ULBE of at 333 K

Table 3: Kinetic parameters for the inhibition of the corrosion of Mild steel in 0.5 M H_2SO_4 solution containing various concentrations of ULBE at different temperature

Conc (g/L)	K (hrs^{-1})				$t_{1/2}$ (hrs)				R^2			
	303K	313K	323K	333K	303K	313K	323K	333K	303K	313K	323K	333K
Blank	0.0048	0.0071	0.0084	0.0087	144.68	97.23	82.40	79.38	0.993	0.949	0.992	0.957
0.2	0.0056	0.0081	0.0088	0.0094	124.42	85.24	78.75	73.96	0.991	0.957	0.993	0.963
0.4	0.0058	0.0083	0.0094	0.0095	119.90	81.59	73.57	72.72	0.996	0.960	0.996	0.968
0.6	0.0060	0.0085	0.0095	0.0097	115.69	81.53	73.18	71.66	0.997	0.972	0.994	0.969
0.8	0.0068	0.0083	0.0096	0.0099	102.36	83.59	72.49	70.28	0.991	0.950	0.991	0.973
1.0	0.0065	0.0082	0.0093	0.0101	107.11	84.31	74.28	68.41	0.993	0.958	0.995	0.966

3.5 Adsorption Isotherm Models

Different isotherm models such as Langmuir, Freundlich, Henry, El-Awady, Flory-Huggins, Frumkin, Temkin and Virial-Parson were used to analyze the adsorption of ULBE on to the mild steel surfaces. The plots of various isotherms models were shown in Figures 13 - 20 while the corresponding Tables obtained from the plots and isotherm parameters were shown in Table 4a-4c. The value of correlation coefficient (R^2) was used to determine the best fit. Langmuir adsorption isotherm model was found to be the best fit for the adsorption of the inhibitor on mild steel. As discussed by several authors, the determination of adsorption parameters, especially, the free enthalpy of adsorption of various components of the natural extracts as well as the known molecule responsible of the inhibition process, but generally explained by the synergistic intermolecular effect of the molecules containing heteroatoms (S, N, O ….) or aromatic rings, doble, triple bonds… which can interact with the metal surface to create a barrier against the arrival of aggressive species like the hydrogen ion in acidic media, we limit our determination to the K_{ads} leading to a negative values of ΔG_{ads} (Benali *et al.*, (2013); Khadom, *et al*. (2022); Sharma *et al*, (2023); Lrhoul, *et al*. (2023)).

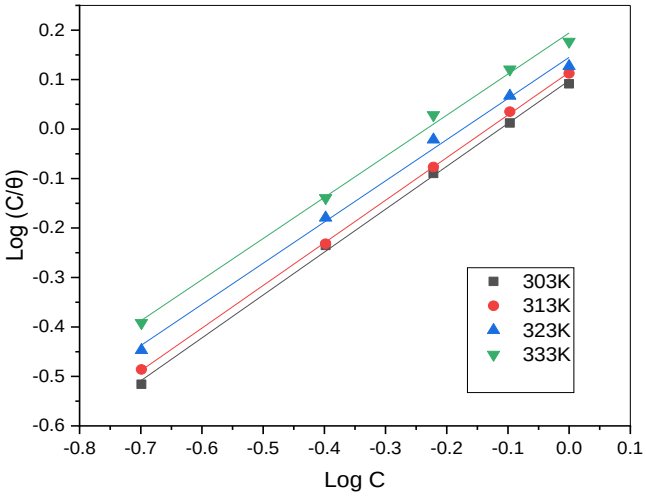

Figure 13: Langmuir isotherm for adsorption of ULBE on MS surface

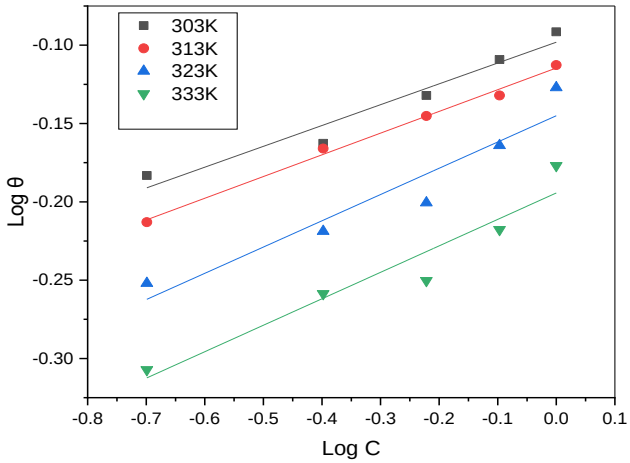

Figure 14: Freundlich isotherm for adsorption of ULBE on MS surface

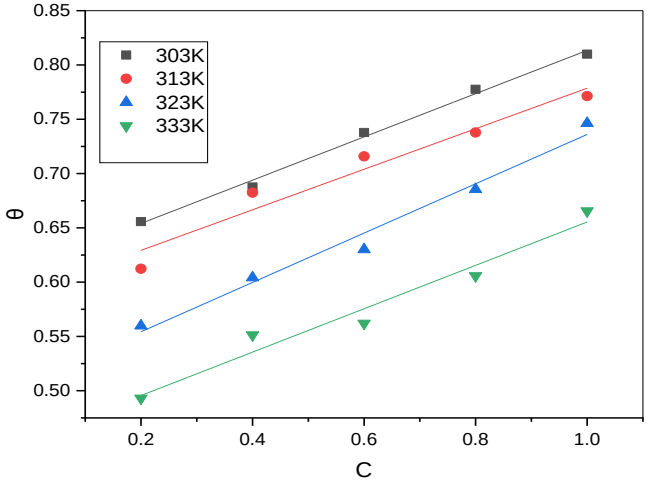

Figure 15: Henry isotherm for adsorption of ULBE on MS surface

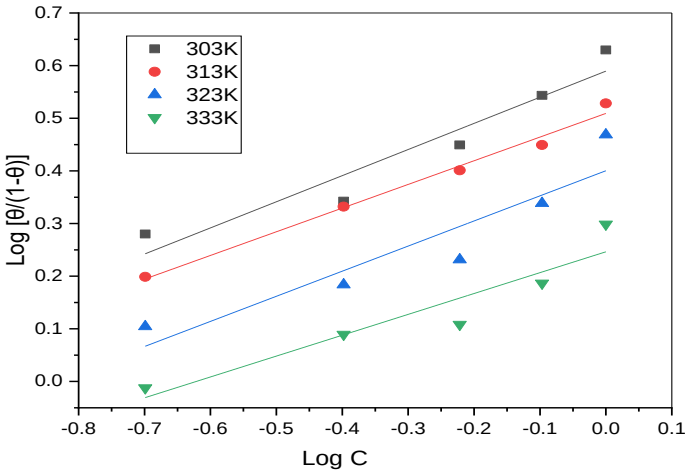

Figure 16: El-Awady for adsorption of ULBE on MS surface

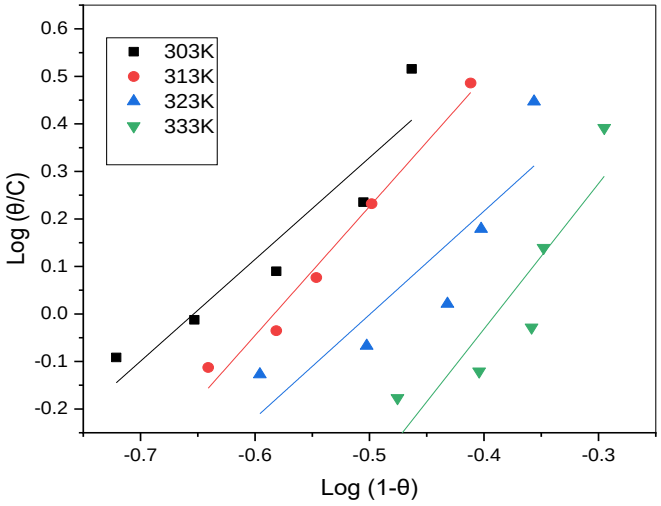

Figure 17: Flory-Huggins for adsorption of ULBE on MS surface

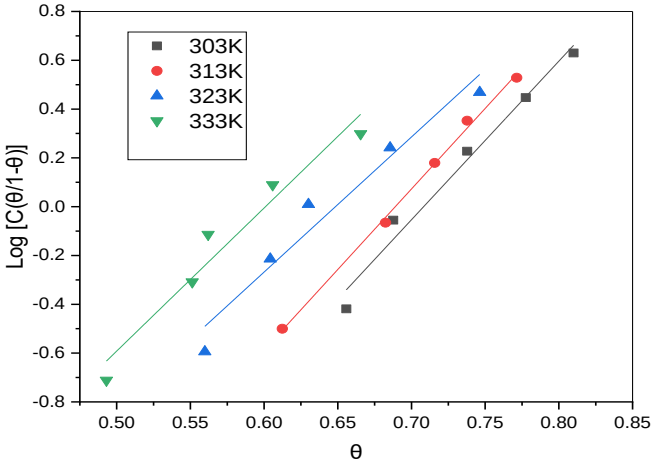

Figure 18: Frumkin for adsorption of ULBE on MS surface

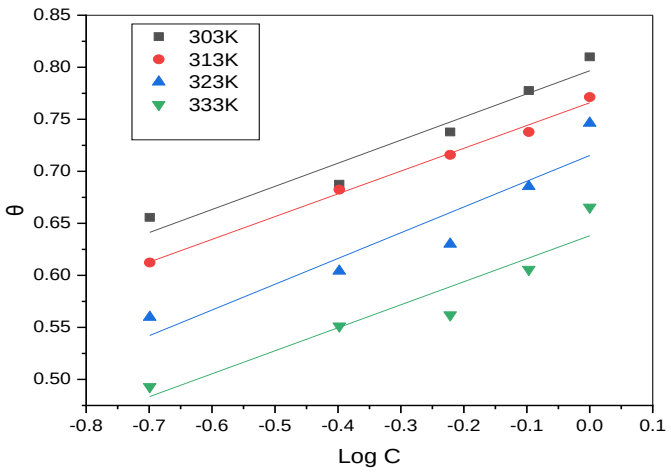

Figure 19: Temkin for adsorption of ULBE on MS surface

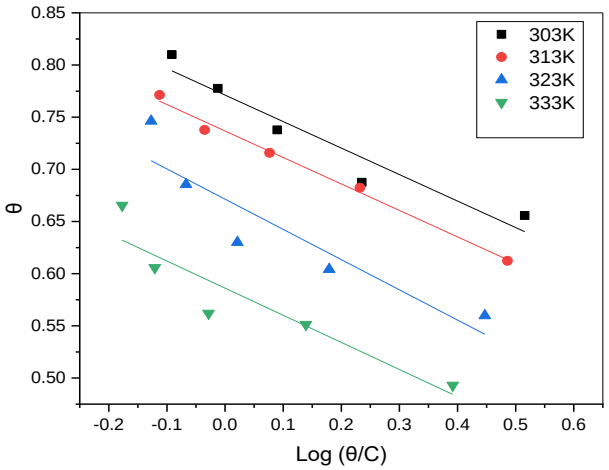

Figure 20: Virial-Parson for adsorption of ULBE on MS surface

Table 4a: Isotherm table for adsorption of ULBE inhibitor on MS surface

Model	T (K)	R^2	Slope	Intercept	K_{ads}
Langmuir	303	0.99	0.87	0.10	0.79
	313	0.99	0.86	0.11	0.77
	323	0.99	0.83	0.15	0.72
	333	0.99	0.83	0.19	0.64
Freundlich	303	0.95	0.13	- 0.10	0.79
	313	0.99	0.14	- 0.11	0.77
	323	0.91	0.17	- 0.15	0.72
	333	0.92	0.17	- 0.19	0.64
Henry	303	0.99	0.19	0.55	0.19
	313	0.95	0.19	0.47	0.19
	323	0.98	0.23	0.39	0.23
	333	0.96	0.19	0.34	0.19

Table 4b: Isotherm table for adsorption of ULBE inhibitor on MS surface

Model	T (K)	R^2	Slope	Intercept	K_{ads}	α
Temkin	303	0.94	0.22	0.79	3846.80	-5.18
	313	0.99	0.22	0.77	3165.92	-5.26
	323	0.89	0.25	0.72	775.71	-4.65
	333	0.89	0.22	0.64	768.78	-5.21
Frumkin	303	0.96	5.02	-2.78	0.062	2.51
	313	0.98	6.49	-4.60	0.010	3.25
	323	0.99	6.59	-4.55	0.011	3.29
	333	0.95	5.53	-3.59	0.028	2.77
Flory- Huggins	303	0.89	2.14	1.40	25.14	2.14
	313	0.98	2.71	1.58	38.33	2.71
	323	0.78	2.18	1.09	12.24	2.18
	333	0.82	3.06	1.19	15.59	3.06

Table 4c: Isotherm table for adsorption of ULBE inhibitor on MS surface

Model	T (K)	R^2	Slope	Intercept	K_{ads}	$\frac{1}{y}$
El-Awady	303	0.9218	0.49648	0.5896	3.8869	2.01
	313	0.9886	0.44975	0.50925	3.2304	2.22
	323	0.8628	0.47704	0.40034	2.5139	2.50
	333	0.8877	0.39632	0.24637	1.7635	1.76
Virial – Parson	303	0.93	-0.25393	0.77119	4.5347	1088.93
	313	0.99	-0.25371	0.73677	4.5386	801.68
	323	0.85	-0.28966	0.67143	3.9754	207.97
	333	0.86	-0.25993	0.58618	4.4300	179.93

3.6 Thermodynamic Evaluation

The enthalpy and entropy of adsorption of ULBE was evaluated using the integrated van't Hoff equation; equation 7 (Ebenso & Obot, (2010); Lai, *et al*. (2017)):

$$\ln K_{ads} = -\frac{\Delta H}{RT} + \frac{\Delta S}{R} - \ln(55.5) \qquad 7$$

The van't Hoff Plot of $\ln K_{ads}$ against $\frac{1}{T}$ is shown in Figure 21 and the calculated values of enthalpy and entropy of adsorption were shown in Table 5. The enthalpies of adsorption of ULBE were - 7.133 kJ/mol. Since the value was negative, it indicates the exothermic process of adsorption. Because ΔH_{ads}value were was less than 40 kJ/mol, it confirms the physical adsorption mechanism of ULBE inhibitor on mild steel (Musa *et al*. (2007)). The adsorption entropy ΔS_{ads} value for the inhibitor on mild steel was 12.339 J/mol/K. Positive values of ΔS_{ads} indicates increase in disorderliness in going from reactants to the mild steel/solution interface (Badiea *et al*. (2009)) resulting in spontaneous process. More so, the negative value of ΔG_{ads} confirms the feasibility and spontaneity of the adsorption inhibition process.

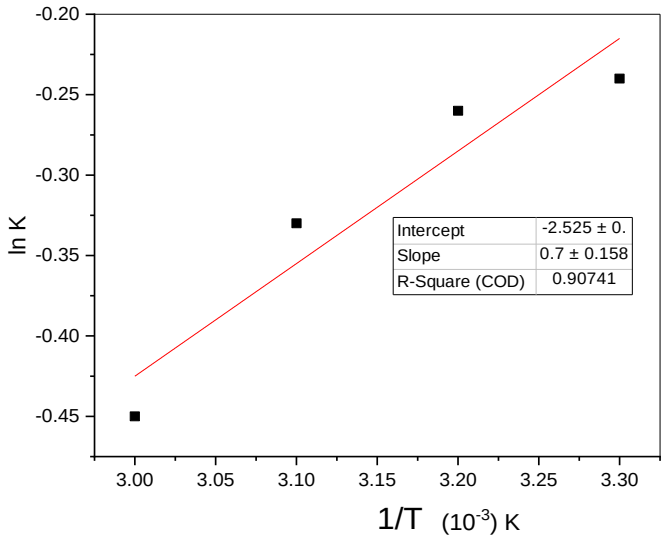

Figure 21: van't Hoff plot of ln K against $\frac{1}{T}$

Table 5: Enthalpy and entropy of adsorption values for the adsorption of ULBE mild steel surface

ΔH°_{ads} (kJ/mol)	ΔS°_{ads} (J/mol/K)
-7.133	12.339

3.7 Surface Morphological Studies

3.7.1 Scanning Electron Microscopy (SEM)

The SEM analysis was carried out on polished mild steel surface immersed for 168 h in 0.5 M H_2SO_4 solution in the presence and absence of ULBE as presented in Figure 22.

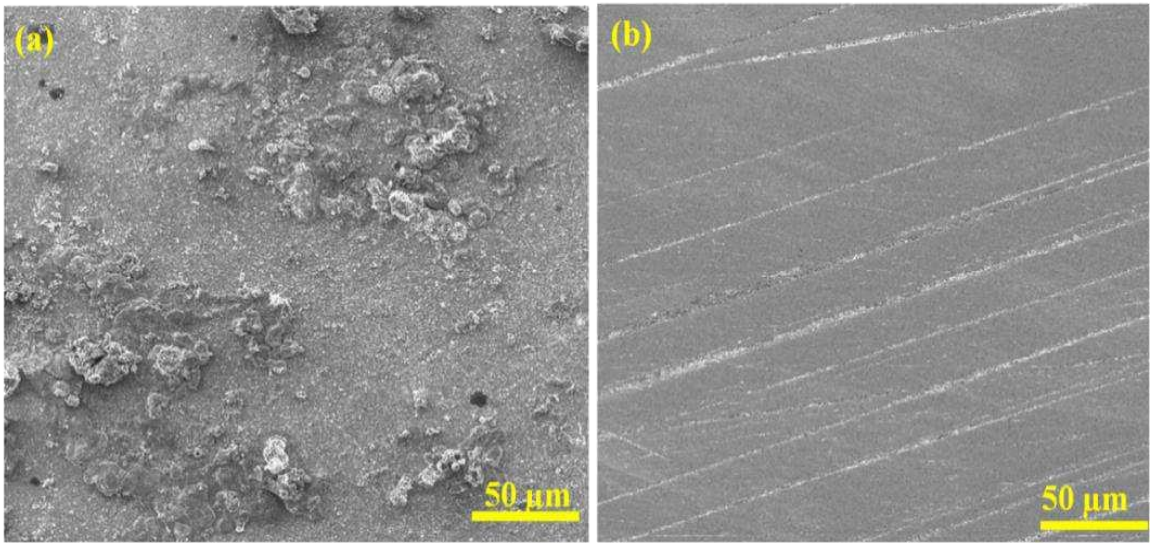

Figure 22: SEM images of mild steel in (a) blank and (b) inhibited by 1.0 g/L ULBE

By comparing the SEM images before and after immersion, mild steel surfaces were strongly damaged in the absence of ULBE inhibitor, which results in heterogeneous and rough surface due to corrosive nature of the H_2SO_4 acid. The SEM images for inhibited solution revealed a smoother surface morphology because of formation of film protective layer of the extract inhibitor molecules on the

surface of the mild steel thereby, inhibiting the corrosion process (Li *et al*. (2009); Enyinnaya *et al*. (2021)).

3.7.2 Fourier Transformation Infrared Spectroscopy (FTIR)

Fourier Transformation Infrared Spectroscopy (FTIR) spectra used to assess the protective film created on the metal surface revealed the bonding type for organic inhibitors adsorbed at the surface the metal (Enyinnaya *et al*. (2021)).

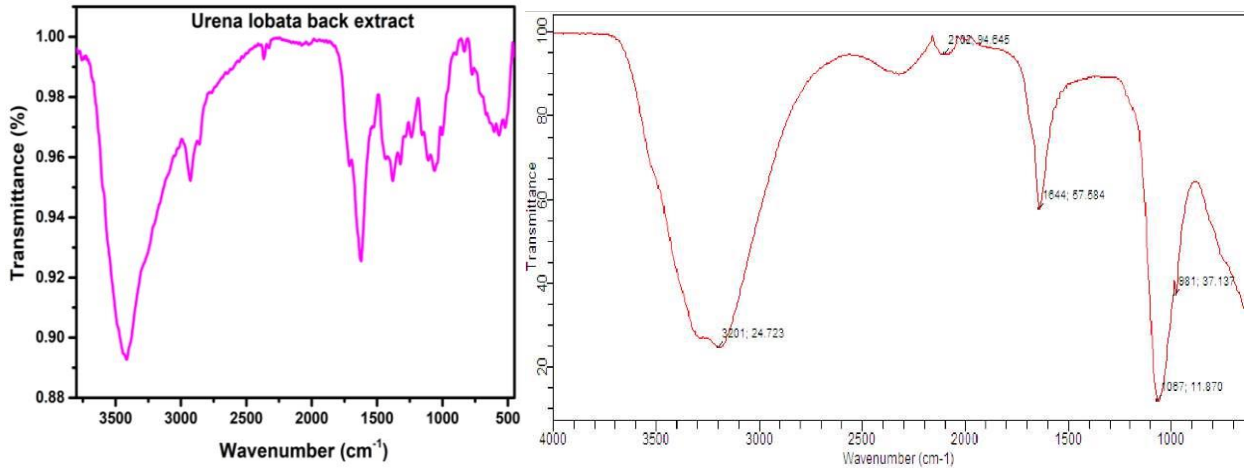

Figure 23: FTIR Spectroscopy of (a) Crude ULBE and (b) washing solution after immersion in 0.5 M H_2SO_4 solution with 1.0 g/L ULBE

Table 6: FTIR Spectra of ULBE

S/No	Wavenumber (cm^{-1})	Functional Group
1	3865.97	O-H stretching of alcohol
2	3415.31	N-H stretching of primary amine
3	2928.00	C-H asymmetric stretching in CH_2
4	2366.95	C-O bond
5	2077.17	C-H bond of aromatic compound
6	1711.30	C=O in carboxylic acid
7	1622.29	C=C vibration
8	1380.24	C-N in amine
9	1322.61	C-H in alkanes
10	1231.45	C-O stretching in ethers
11	1108.22	C-O in esters
12	1002.46	C-O in esters
13	833.11	N-H bending
14.	712.13	C=C bending alkenes
15.	685.54	C-H sharp

The results shown in Figure 23 and Table 6 revealed the presence of many active functional groups like ketones, aldehydes, amines, amides, alcohols, alkenes, alkynes, and aromatics, which have corrosion inhibitory properties. A shift of the spectra after 168 hr of immersion was due to interactions between the mild steel and the inhibitor's molecules resulting in inhibition. These interactions were

also responsible for the disappearance of some functional groups because of their adsorption on the mild steel surface (Ojha *et al*. (2017)).

Conclusion

This study revealed that the inhibition efficiency of ULBE increased with increase in concentration and maximum efficiency of 96.82% was observed at 1.0 g/L and 303 K. Inhibition efficiency also decreased with temperature rise from 303 K to 333 K. The results of thermodynamic, kinetics and thermochemical parameters obtained showed that the mechanism of adsorption of ULBE on mild steel surface was physical. It further revealed that adsorption of ULBE molecules on mild steel surface was exothermic, feasible, spontaneous and best fitted the Langmuir adsorption isotherm model. The Scanning Electron Micrograph and Fourier Infra-red spectra supported the formation of adsorption film on mild steel surface which reduced the exposed surface area thereby inhibiting corrosion. The results obtained in this study showed that *Urena lobata* bark extract (ULBE) could act as an effective corrosion inhibitor for corrosion mitigation of mild steel in 0.5 M sulphuric acid.

Statements and Declarations

The authors state that the work is an original blue-print and has not been published elsewhere or under any kind of review.

Conflicting Interest

The authors declare no competing academic and financial interests

References

Abakedi O. U., Moses I. E., & Asuquo J. E. (2016). Adsorption and inhibition effect of *Maesobatrya barteri* leaf extract on aluminium corrosion in hydrochloric acid solution. *Journal* of *Scientific* and *Engineering* Research *3*(1), 138-144.

Abdallah M., Gad E. A. M., Sobhi M., Al-Fahemi J. H., & Alfakeer M. M. (2019). Performance of tramadol drug as a safe inhibitor for aluminum corrosion in 1.0 M HCl solution and understanding mechanism of inhibition using DFT. *Egyptian Journal of Petroleum*, *28*(2), 173-181. https://doi.org/10.1016/j.ejpe.2019.02.003

Akpan E. D., Singh A. K., Lgaz H., Quadri T. W., Shukla S. K., Mangla B., Dwivedi A., Dagdag O., Inyang E. E. & Ebenso, E. E. (2024). Coordination compounds as corrosion inhibitors of metals: A review. *Coordination Chemistry Reviews*, *499*, 215503. https://doi.org/10.1016/j.ccr.2023.215503

Awe F. E., Idris S. O., Abdulwahab M., & Oguzie E. E. (2015). Inhibitive and adsorptive effect of *Parinari polyandra* on mild steel corrosion in aqueous sulphuric acid. *African Journal of Pure and Applied Chemistry*, *9*(6), 125-134. http://dx.doi.org/10.5897/AJPAC2015.0630

Badiea A. M., Mohana K.N. (2009). Effect of temperature and fluid velocity on corrosion mechanism of low carbon steel in presence of 2-hydrazino-4, 7-dimethylbenzothiazole in industrial water medium. *Corrosion Science*, *51*(9), 2231-2241. https://doi.org/10.1016/j.corsci.2009.06.011

Banu K. S., & Cathrine L. (2015). General techniques involved in phytochemical analysis. *International Journal of Advanced Research in Chemical Science*, *2*(4), 25-32.

Benali O., Benmehdi H., Hasnaoui O., Selles C., Salghi R. (2013). Green corrosion inhibitor: inhibitive action of tannin extract of Chamaerops humilis plant for the corrosion of mild steel in 0.5 M H_2SO_4, *J. Mater Environ. Sci,* 4 (1), pp. 127-138

Bentiss F., Lebrini M., Vezin H., Chai F., Traisnel M., & Lagrené M. (2009). Enhanced corrosion resistance of carbon steel in normal sulfuric acid medium by some macrocyclic polyether compounds containing a 1, 3, 4-thiadiazole moiety: AC impedance and computational studies. *Corrosion science*, *51*(9), 2165-2173.

Bouklah M., Hammouti B., Lagrenee M., & Bentiss F. (2006a). Thermodynamic properties of 2, 5-bis (4-methoxyphenyl)-1, 3, 4-oxadiazole as a corrosion inhibitor for mild steel in normal sulfuric acid medium. *Corrosion Science*, *48*(9), 2831-2842. https://doi.org/10.1016/j.corsci.2005.08.019

Bouklah M., Ouassini K., Hammouti B., El Idrissi A. (2006b), Corrosion inhibition of steel in sulphuric acid by pyrrolidine derivatives, *Appl. Surf. Sci.*, 252 N°6, 2178-2185.

Chaubey N., Savita Singh, V. K., & Quraishi M. A. (2017). Corrosion inhibition performance of different bark extracts on aluminium in alkaline solution. *Journal of the Association of Arab Universities for Basic and Applied Sciences*, *22*(1), 38-44. https://doi.org/10.1016/j.jaubas.2015.12.003

Chetouani A., K. Medjahed, K.E. Sid-Lakhdar, B. Hammouti, M. Benkaddour, A. Mansri (2004), Poly(4-vinylpyridine poly(3-oxide ethylene) tosyle) an excellent inhibitor for iron in sulphuric acid medium at 80°C. *Corros. Sci.*, 46, 2421-2430.

Dhakal K., Bohora D., Bista B., Oli H., Singh S., Bhattarai D., Karki N. & Yadav A. (2022). Alkaloids extract of *Alnus nepalensis* bark as a green inhibitor for mild steel corrosion in 1 M H_2SO_4 solution. *Journal of Nepal Chemical Society*, *43*(1), 76-92. http://dx.doi.org/10.3126/jncs.v43i1.46999

Diki N. Y. S., Bohoussou K. V., Kone M. G. R., Ouedraogo A., & Trokourey A. (2018). Cefadroxil drug as corrosion inhibitor for aluminum in 1 M HCl medium: experimental and theoretical studies. *IOSR Journal of Applied Chemistry*, *11*(4), 24-36.

Ebenso E. E., & Obot I. B. (2010). Inhibitive properties, thermodynamic characterization and quantum chemical studies of secnidazole on mild steel corrosion in acidic medium. *International Journal of Electrochemical Science*, *5*(12), 2012-2035. http://dx.doi.org/10.1016/S1452-3981(23)15402-2

Enyinnaya N. P., James A. O., & Obi C. (2021). Corrosion inhibition of *Urena lobata* leaves extract on mild steel corrosion in H_2SO_4 acid. *International Journal of advances in Engineering and Management*, *3*(12), 1275-1286. http://dx.doi.org/10.35629/5252-031212751286

Enyinnaya N. P., James A. O., & Obi C. (2022). Inhibitive potential of benign Caesar-weed leaves extract (CWLE) as corrosion inhibitor of aluminium in H_2SO_4 phase. *Interdisciplinary Journal of Applied and Basics Subjects*, *2*(1), 1-13.

Feng Y., He J., Zhan Y., An J., & Tan B. (2021). Insight into the anti-corrosion mechanism Veratrum root extract as a green corrosion inhibitor. *Journal of Molecular Liquids*, *334*, 116110. https://doi.org/10.1016/j.molliq.2021.116110

Fouda A. S., Al-Sarawy A. A., & El-Katori E. E. (2006). Pyrazolone derivatives as corrosion inhibitors for C-steel in hydrochloric acid solution. *Desalination*, *201*(1-3), 1-13. http://dx.doi.org/10.1016/j.desal.2006.03.519

Fouda A. S., Killa H. M., Farouk A., Salem A.M. (2019) Calicotome extract as a friendly corrosion inhibitor for Carbon steel in polluted NaCl Solution: Chemical and Electrochemical studies. *Egyptian Journal Chem.*, *62*(10), 1879-1894. https://doi.org/10.21608/ejchem.2019.7656.1649

Ghazi Z., ELmssellem H., Ramdani M., Chetouani A., Rmil R., Aouniti A., & Hammouti B. (2014). Corrosion inhibition by naturally occurring substance containing *Opuntia-Ficus Indica* extract on the corrosion of steel in hydrochloric acid. *Journal of Chemical* and *Pharmaceutical Research 6*, 1417-1425.

Guo L., Kaya S., Obot I. B., Zheng X., & Qiang Y. (2017). Toward understanding the anticorrosive mechanism of some thiourea derivatives for carbon steel corrosion: A combined DFT and molecular dynamics investigation. *Journal of colloid and interface science*, *506*, 478-485. https://doi.org/10.1016/j.jcis.2017.07.082

Haldhar R., Prasad D., Saxena A., Singh P. (2018). *Valeriana wallichii* root extract as a green & sustainable corrosion inhibitor for mild steel in acidic environments: experimental and theoretical study. *Materials Chemistry Frontiers*, *2*(6), 1225-1237. http://dx.doi.org/10.1039/C8QM00120K

Hammouti B., A Zarrouk, SS Al-Deyab, Warad I. (2013) Temperature Effect, Activation Energies and Thermodynamics of Adsorption of ethyl 2-(4-(2-ethoxy-2-oxoethyl)-2-p-Tolylquinoxalin-1 (4H)-yl) Acetate on Cu in HNO3 *Oriental Journal of Chemistry* 27 (1), 23-31

Hanoon M. M., Resen A. M., Shaker L. M., Kadhum A. A. H., & Al-Amiery A. A. (2021). Corrosion investigation of mild steel in aqueous hydrochloric acid environment using n-(Naphthalen-1yl)-1-(4-pyridinyl) methanimine complemented with antibacterial studies. *Biointerface Res. Appl. Chem*, *11*(2), 9735-9743.

Ijuo G. A., Orokpo M. A., Surma N., & Tor P. N. (2018). Methanol extract of *Canarium sweinfurthii* as a green inhibitor for the corrosion of mild steel in HCl: adsorption, kinetic, thermodynamic and synergistic studies. *Journal* of Materials and *Environmental Science 9*, 3113-3123

Jisha M., Hukuman N. Z., Leena P., & Abdussalam A. K. (2019). Electrochemical, computational and adsorption studies of leaf and floral extracts of *Pogostemon quadrifolius* (Benth.) as corrosion inhibitor for mild steel in hydrochloric acid. *Journal of Materials and Environmental Science 10*(9), 840-853.

Khadom A. A., Abd, A. N., Ahmed, N. A. (2022). Synergistic effect of iodide ions on the corrosion inhibition of mild steel in 1M HCl by Cardaria Draba leaf extract, *Results in Chemistry*, 4, 100668, ISSN 2211-7156, https://doi.org/10.1016/j.rechem.2022.100668

Kikanme N. K., James A. O., & Ngobiri N. C. (2020). *Vigna unguiculata* coat extract as green corrosion inhibitor for steel Pipeline in HCl. *Journal of Materials Science Research and Reviews*, *5*(1), 5-1.

Lai C., Xie B., Zou L., Zheng X., Ma X., & Zhu S. (2017). Adsorption and corrosion inhibition of mild steel in hydrochloric acid solution by S-allyl-O, O′-dialkyldithiophosphates. *Results in physics*, *7*, 3434-3443. https://doi.org/10.1016/j.rinp.2017.09.012

Li X., Deng S., Fu H., & Li T. (2009). Adsorption and Inhibition effect of 6-benzylaminopurine on cold rolled steel in 1.0 M HCl. *Electrochimica Acta*, *54*(16), 4089-4098. https://doi.org/10.1016/j.electacta.2009.02.084

Lrhoul H., Sekkal H., Hammouti B. (2023) Natural Plants as Corrosion Inhibitors: Thermodynamic's restrictions, *Mor. J. Chem.*,14(3), 689-698, https://doi.org/10.48317/IMIST.PRSM/morjchem-v11i3.40144

Ma I. W., Ammar S., Kumar S. S., Ramesh K., & Ramesh S. (2022). A concise review on corrosion inhibitors: types, mechanisms and electrochemical evaluation studies. *Journal of Coatings Technology and Research*, 1-28. https://doi.org/10.1007/s11998-021-00547-0

Musa A. Y., Kadhum A. A. H., Mohamad A. B., Daud A. R., Takriff M. S., & Kamarudin S. K. (2009). A comparative study of the corrosion inhibition of mild steel in sulphuric acid by 4, 4-dimethyloxazolidine-2-thione. *Corrosion science*, *51*(10), 2393-2399. https://doi.org/10.1016/j.corsci.2009.06.024

Ngobiri N. C., & Obi C. (2020). Corrosion inhibition behaviour of *Enantia chlorantha* extract on pipeline steel corrosion in acidic system. *Journal of Applied Sciences and Environmental Management*, *24*(4), 707-712. http://dx.doi.org/10.4314/jasem.v24i4.24

Ojha L. K., Kaur K., Kaur R., & Bhawsar J. (2017). Corrosion inhibition efficiency of fenugreek leaves extract on mild steel surface in acidic medium. *Journal of Chemical and Pharmaceutical Research*, *9*(6), 57-67.

Popov B. N. (2015). Corrosion Engineering: principles and solved problems. Elsevier

Revie R. W., & Uhlig H. H. (2008). Corrosion and corrosion control: an introduction to corrosion science and engineering. John Wiley and Sons, New Jersey.

Saeed M. T., Saleem M., Usmani S., Malik I. A., Al-Shammari F. A., & Deen K. M. (2019). Corrosion inhibition of mild steel in 1 M HCl by sweet melon peel extract. *Journal of King Saud University-Science*, *31*(4), 1344-1351.https://doi.org/10.1016/j.jksus.2019.01.013

Santhini N., & Jeyaraj T. (2012). The inhibition effect of [3-(4-hydroxy-3-methoxy-phenyl)-1-phenyl-propenone] on the corrosion of the aluminium in alkaline medium. *Journal of Chemical* and *Pharmaceutical Research 4*(7), 3550-3556.

Sharma N., Kumar S., Thakre G.D., Ray A. (2023). Triangle Ester' Molecules as Blending Components in Mineral Oil: A Theoretical and Experimental Investigation. *Lubricants,* 11,144. https://doi.org/10.3390/lubricants11030144

Sulay Z. K., Victor A. U., Obed B., & Olufemi A. O. (2015). Kinetics and thermodynamic study of inhibition potentials by ethoxyethane extracts of *Cochlospermum tinctorium* for the oxoacid corrosion of mild steel. *International Journal* of Materials and *Chemistry 5*(3), 64-76. http://dx.doi.org/10.5923/j.ijmc.20150503.03

Umoren S. A., Abdullahi M. T., & Solomon M. M. (2022). An overview on the use of corrosion inhibitors for the corrosion control of Mg and its alloys in diverse media. *Journal of Materials Research and Technology*, *20*, 2060-2093. https://doi.org/10.1016/j.jmrt.2022.08.021

Zarrok H., Zarrouk A., Salghi R., M. Assouag, B. Hammouti, H. Oudda, S. Boukhris, S. S. Al Deyab, I. Warad (2013), Inhibitive properties and thermodynamic characterization of quinoxaline derivative on carbon steel corrosion in acidic medium, *Der Pharma Lettre,* 5 (2) 43-53